

Self-organized pore formation and open-loop-control in semiconductor etching

Jens Christian Claussen^{1,2}, Jürgen Carstensen¹, Marc Christophersen¹, Sergiu Langa¹, and Helmut Föll¹

¹Chair for general materials science, CAU University of Kiel, Kaiserstr. 2, 24143 Kiel, Germany

<http://www.tf.uni-kiel.de/matwis/amat/>

²Theoretische Physik und Astrophysik, Universität Kiel, Leibnizstr. 15, 24098 Kiel, Germany

<http://www.theo-physik.uni-kiel.de/~claussen/>

Published in *CHAOS (AIP)* 13 (1), 217-224 (2003)

Abstract

Electrochemical etching of semiconductors, apart from many technical applications, provides an interesting experimental setup for self-organized structure formation capable e.g. of regular, diameter-modulated, and branching pores. The underlying dynamical processes governing current transfer and structure formation are described by the Current-Burst-Model: all dissolution processes are assumed to occur inhomogeneously in time and space as a Current Burst (CB); the properties and interactions between CB's are described by a number of material- and chemistry-dependent ingredients, like passivation and aging of surfaces in different crystallographic orientations, giving a qualitative understanding of resulting pore morphologies. These morphologies cannot be influenced only by the current, by chemical, material and other etching conditions, but also by an open-loop control, triggering the time scale given by the oxide dissolution time. With this method, under conditions where only branching pores occur, the additional signal hinders side pore formation resulting in regular pores with modulated diameter.

Silicon monocrystals are the most perfect material mankind has ever created since they are essential for high integrated computer circuits. Due to this high degree of perfection, i. e. corrosion is not defect-driven, and “ideal corrosion” is possible: Silicon and other semiconductors can be made porous by electrochemical etching giving an outstanding variety of pore sizes, from nanopores to macropores, and geometries, including disordered nanoporous, dendritic-like sidebranching pores, and pores with modulated diameter. Abstracting from the details of the underlying electrochemical processes, the Current Burst Model together with the Aging Concept, and accounting the interactions between Current Bursts, the generation of different pore geometries, oscillations and synchronization phenomena can be explained including the percolation transition to global oscillations. Based on the time scale derived from the Aging Concept, an open-loop control can be applied to suppress sidebranching of pores in a technologically relevant regime.

1 Introduction

The solid - liquid junction of Silicon and HF - containing liquids exhibits a number of peculiar features, e.g. a very low density of surface states, i.e. an extremely well “passivated” interface [1]. If the junction is biased, the IV - characteristics (Fig. 1) in diluted HF is quite complicated and exhibits two current peaks and strong current- or voltage oscillations at large current densities (for reviews see [2, 3]). These oscillations have been described quantitatively by the Current-Burst-Model [4, 5, 6, 7].

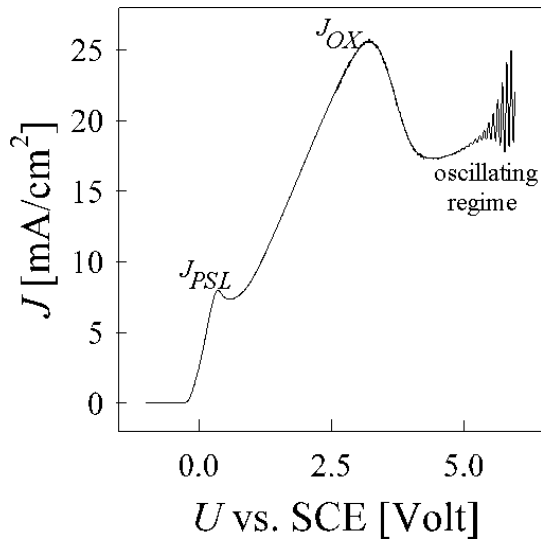


Figure 1: The IV- characteristics of the silicon-hydrofluoric acid contact shows different phenomena from generation of a porous silicon layer (PSL), oxidation and electropolishing (OX) and electrochemical oscillations at higher anodic bias.

Perhaps the most outstanding features are the many different kinds of pores - nanopores, mesopores, macropores, and so on - that form under a wide range of conditions in many HF containing electrolytes, including organic substances [8, 9]. Despite of an intensive research triggered by the finding that nanoporous Si shows strong luminescence [10, 11], neither the intricacies of the IV - characteristics nor the processes responsible for the formation of pores,

including their rather peculiar dependence on the crystal orientation, are well understood.

Replacing Si by III/V-compounds, a variety of different pore morphologies can be etched; due to different properties of the A- and B- surfaces one finds e.g. tetrahedron-shaped pores instead of octahedron-shaped pores. For an overview over recent results see [12]. But again most of the phenomenon can be well understood within the framework of the Current-Burst-Model which seems to reflect a number of quite general properties of semiconductor electrochemistry.

2 Experimental Setup and Basic IV Characteristics

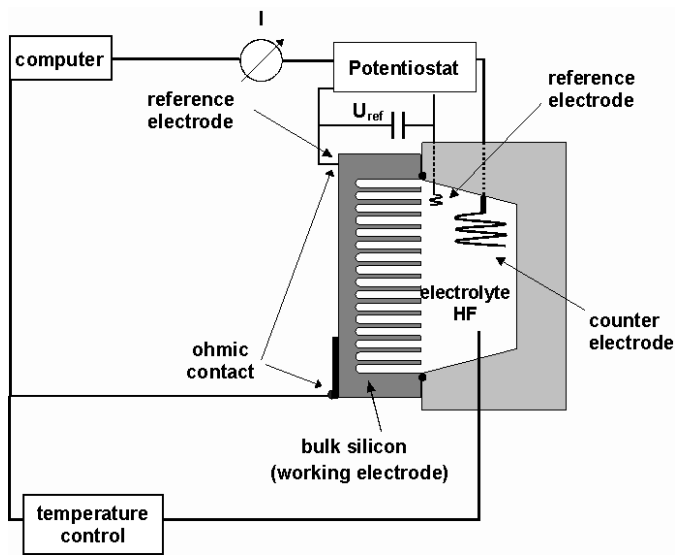


Figure 2: The experimental set-up used for electrochemical anodization of semiconductors.

The basic setup is shown in Fig. 2. Using a four electrode arrangement a potentiostat/galvanostat is contacting the sample and the electrolyte, allowing for a well defined potential resp. current for the electrochemical dissolution reactions. Since the potentiostat/galvanostat as well as the temperature are PC controlled, all relevant etching parameters can be controlled in detail. While the principal setup remains the same in all experiments, backside contact, front- and/or backside illumination and electrolyte pumping can be varied as well as cell size (from under 0.3 cm up to wafers of 6 in) and semiconductor material (Si, InP, GaAs, GaP) including various doping levels and crystallographic orientations. In addition, the electrolytes (e.g. HF, HCl, H₂SO₄) and their concentrations and temperature can be varied.

3 The Current-Burst Model

The Current Burst Model [4, 5, 6, 13] states that the dissolution mainly takes place on small spots in short events, starting with a direct Si-dissolution, and possibly followed by an oxidizing reaction (see Fig. 3).

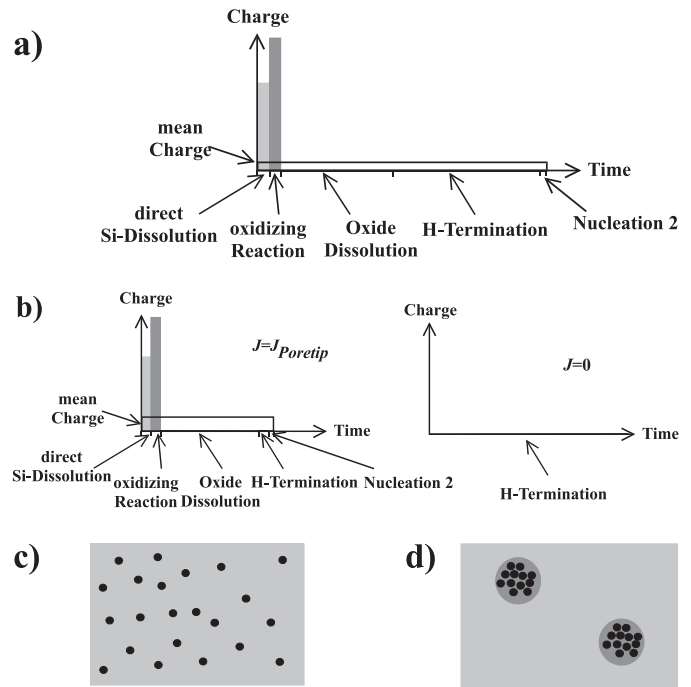


Figure 3: Applying a global current density smaller than the average current density in a current burst will either require very long time constants to keep the mean charge density passed in a burst small and to cover the surface completely with current lines (a), a statistical arrangement of current lines with the optimized (smaller) time constant of the system, leaving parts of the surface without current and creating nanopores (b, c), or induces a phase separation by rearranging the current lines in areas corresponding to macropores (d).

After these two short processes, the oxide hump undergoes dissolution, a time-consuming process which ensures at the location of the current burst a dead-time of fixed length during which no new burst can start. However, immediately after dissolution the Si surface has the highest reactivity, resulting in a maximal probability of another current burst. Due to H-termination the surface becomes passivated, and the probability for bursts decays until it reaches the properties of a completely passivated Si surface, comparable to the situation before the nucleation of the first Current Burst.

This approach allows to connect the average current density \bar{j} with a series of charge and time consuming processes

$$\bar{j} = \frac{\sum Q_i}{\sum \tau_i}. \quad (1)$$

For most of these processes the dependence on the choice of the etching conditions is known; so by “designing” the electrochemical etching conditions (electrolyte, current density, applied voltage, temperature, illumination,...) the properties and interactions of the basic etching process can be tailored to create various pore morphologies. In addition (1) directly couples the local average current density \bar{j} to an intrinsic time constant $\sum \tau_i$. The influence of both, current density and intrinsic time constant, can be measured independently in experiments. Independent

measurements can be described with the same set of parameters. Within the current burst model pore formation from the nm to the μm range as illustrated by Fig. 3 c+d is very easy to describe because the separation of the dissolution processes and the surface passivation processes is already an immanent property of each dissolution cycle, i.e. current burst.

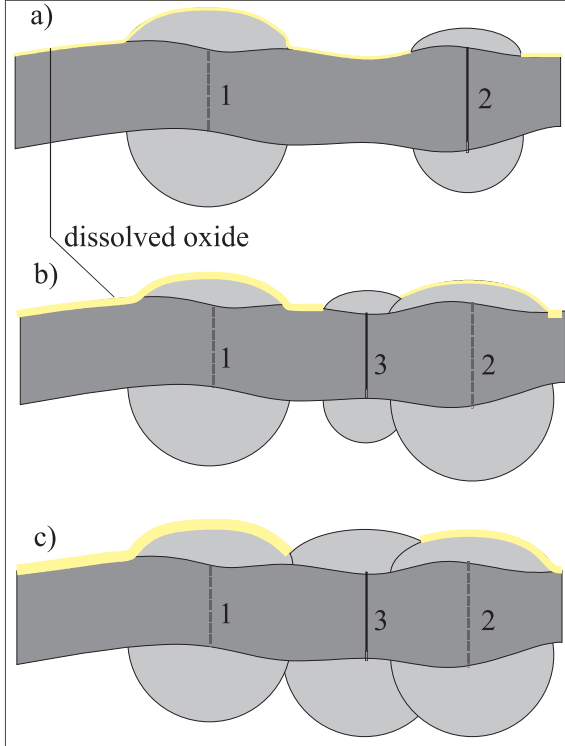


Figure 4: Schematic view of a “ionic breakthrough”. Due to the oxidizing current a roughly semi-spherical oxide inclusion is growing from the tip of channel 1. This is the situation of extremely high current (electrochemical oscillations).

4 Smoothing effect of Oxide Layers and global current oscillations

Depending on the regime in the IV-curve, Current Bursts and their interaction play different roles: For extremely high currents, in the oscillation regime, one has a permanent oxide coverage, and due to the high forcing of the system current bursts are started at all locations where the oxide layer is sufficiently thin for a breakthrough (Fig. 4). In this regime, a detailed Monte Carlo study [5, 6, 7] including the lateral interaction between Current Bursts (overlap of the oxide humps of neighboring Current Bursts) has shown that the Current Burst Model quantitatively can explain the experimental observations of globally oscillating etching current. Due to a phase synchronization of neighboring Current Bursts oxide domains are formed. The size of this domains increases with increasing oxide generation/reduced oxide dissolution. At a percolation point only one oxide domain exists on the sample surface with a synchronized cycle of oxide growth and dissolution,

resulting in a macroscopic oscillation of the external current. The size of the domains as well as the oscillation time can be controlled by the chemical parameters. Even without global oscillations for all regions of the IV-curve where oxide is formed one finds domains of synchronized oxide growth which define the length scale for the roughness of the electrochemically polished sample surface and thus lead to a smoothing of the surface.

5 Passivation Effects: The Aging Concept

While at high current densities the semiconductor surface is completely covered with oxide at low current densities, most of the semiconductor surface will be in direct contact to the electrolyte. It is well known [1] that after chemical dissolution the free surface is passivated, i.e. the density of surface states reduces as a function of time which increases the stability of the surface against further electrochemical attack. Schematically the perfection of the surface passivation and the resulting reduction of the probability for a chemical attack as a function of time are plotted in Fig. 5. For the example of silicon the speed and the perfection of passivation of the (111) crystallographic surface is larger than for the (100) surface. This selective aging of surfaces leads to a self amplifying dissolution of (100) surfaces (which will become pore tips) and a preferential passivation of (111) surfaces (which will become pore walls). Under optimized chemical conditions with an extremely large passivation difference between (111) and (100) surfaces a self organized growth of octahedral cavities occurs as is schematically drawn in Fig. 6. The octahedra consists of (111) pore walls. As soon as the complete surface of the octahedra reaches a critical value, it is easier to start a new cavity at a (100) tip of the old cavity, since the current density in the new, small cavity is larger and no surface passivation will occur until the surface again becomes to large. This growing mechanism leads to an oscillation of both the current through each pore and the diameter of each pore as a function of time which is also plotted in Fig. 6. As in the case of oxide dissolution an internal time constant is related to the pore growth.

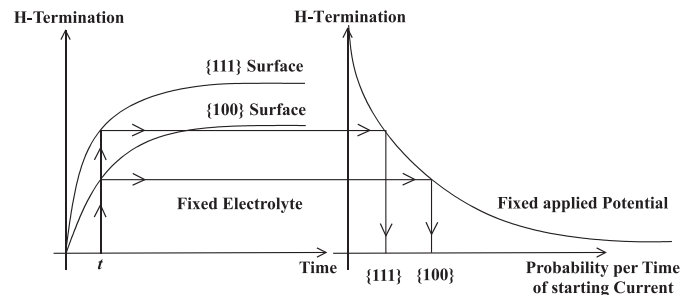


Figure 5: Time constant and perfection of H-termination differ strongly for (100) and (111) Si surface orientation. This leads to an increased probability of local current nucleation on (100) surfaces.

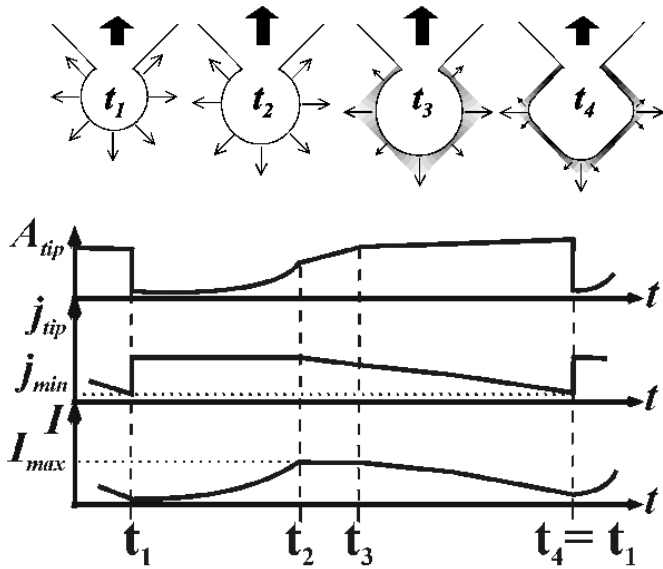


Figure 6: A consequence of the crystallographic dependence of the surface passivation in Fig. 5 is the growth of octahedra like pores. This pore growth is associated with an oscillation of the current through this pore, even for a fixed externally applied potential.

If a global current density smaller than the average current density in a current burst is applied, the aging concept becomes essential to explain the generation of macropores: At passivated surfaces, the nucleation probability of new current bursts is lower than at sites where a current burst has taken place before. Therefore the situation shown in Fig. 3(c) is much more unlikely than the situation shown in Fig. 3(d), so that the whole surface separates in two phases with current-carrying pores and passivated surface without contributions to the total current.

6 Consequences on Pore Geometries

As described above, two synergetic effects occur as a consequence of the interaction of Current Bursts:

- A surface smoothing due to the dissolution of an isotropic oxide layer.
- A strongly anisotropic dissolution of the semiconductor due to the crystallography dependent aging of surfaces which is one of the most important reasons for pore formation.

Depending on the electrochemical composition of Current Bursts the one or the other effect will dominate, and thus may lead to complete different surface morphologies when changing the electrochemical etching conditions; e.g. in a Si-HF-organic electrolyte system only by increasing the HF concentration (i.e. faster oxide dissolution and thus reduced influence of oxide) the electrochemical etching changes from electropolishing (strong oxide smoothing) over macropore formation (pores with diameters of several μm and smooth pore walls) to mesopore formation

(strongly anisotropic, narrow pores with diameters of less than 400nm) [14].

Silicon has one of the most stable oxides of all semiconductors. So for all other semiconductors the smoothing effect is reduced, leading generally to rougher surfaces and smaller pore diameters. In addition the surface aging of III-V compounds is more complicated, since there exist two different (111) surfaces; e.g. in GaAs only the $\{111\}$ A planes (Ga-rich planes) appear as stopping planes. So in most III-V compounds not octahedra (eight (111) surfaces as stopping planes) as in silicon are etched but tetrahedra with only four (111)A surfaces as stopping planes, and the $\{111\}$ B planes (As-rich) serve as preferential growing directions like the (100) directions in Si (see Fig. 7).

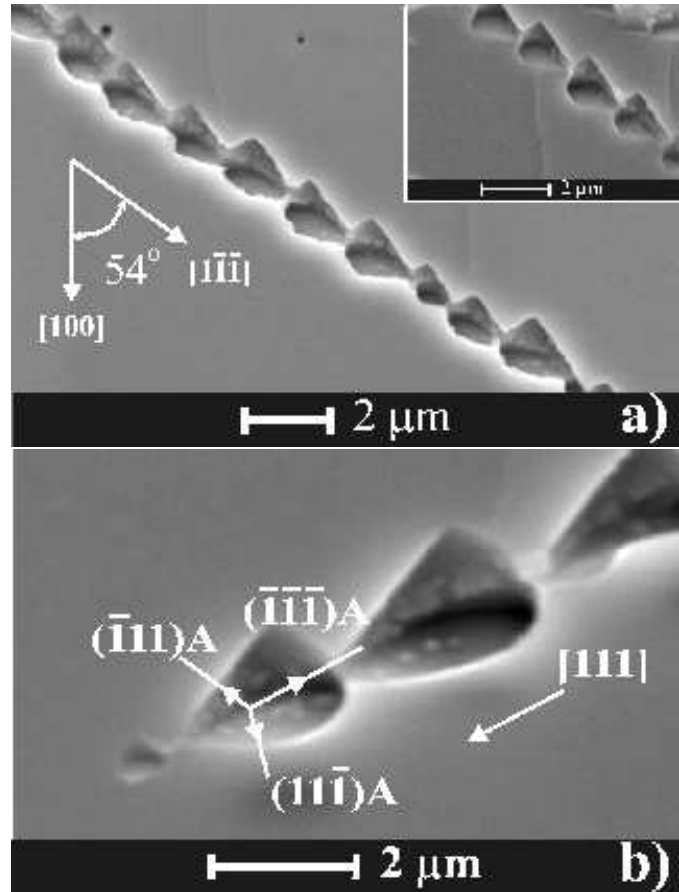


Figure 7: Tetrahedron-like pores oriented along $\langle 111 \rangle$ directions obtained in (100)-oriented n-GaAs ($n = 10^{17} \text{ cm}^{-3}$) at high current density (85 mA/cm^2 , galvanostatic) in HCl (5%) electrolyte.

7 Lateral Interaction of Pores

In the case of stable pore growth active current bursts only exist at each pore tip, so there is no way that current burst can interact directly, e.g. by overlapping. Since several types of pores grow by forming chains of interconnected cavities, i.e. a self induced

diameter modulation is an intrinsic feature of such pores, they can interact indirectly via the space charge region between pores. The serial resistance R of each pore can be described by

$$R(t) = \frac{\rho(t)l(t)}{A(t)} \quad (2)$$

where $\rho(t)$ is the effective specific resistance at a pore tip, $l(t)$ the length of the pore and $A(t)$ the chemically active area at the pore tip. Due to aging $\rho(t)$ will periodically increase and decrease while the cavities are formed. The electric circuit consisting of a parallel connection of large numbers of individually oscillating pores is illustrated in Fig. 8. The consequences for the pore morphologies de-

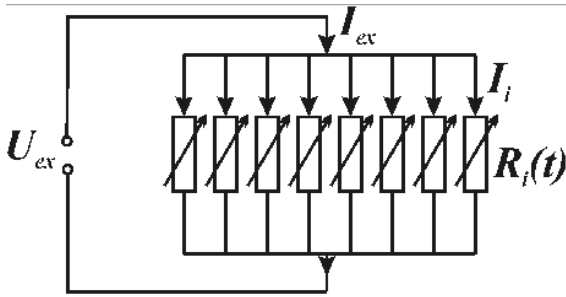


Figure 8: A schematic representation of pores as oscillating resistors in an equivalent circuit diagram.

pend strongly on the etching conditions as schematically illustrated in Fig. 9. At constant voltage condition (potentiostatic control) the current through each pore will be modulated; since the pores grow independently of each other there exists no phase coupling and the overall current is constant.

For galvanostatic control we have to distinguish between two cases:

- At low pore densities (low external current density) there is no restriction for the diameter of the pores; i.e. the area $A(t)$ may increase freely.
- At high pore densities (high external current density) the increase of the diameter is restricted by the neighboring pores; thus the area $A(t)$ is limited.

In the first case we will find diameter modulation (cf. Fig. 9 b)), but still no phase coupling between pores. In the second case the area of the pores can not increase freely to compensate for the reduced effective specific resistance $\rho(t)$. Thus the external voltage must increase to guarantee a constant external current. The voltage increase should synchronize the phases of growth for all pores. This is exactly what is found when, e.g., etching InP at very high current densities. In Fig. 10 a) self induced voltage oscillations are shown which coincide with a simultaneous

diameter increase of all pores (cf. the cross section of the pores in Fig. 10 b)). Obviously not all cycles of the pore growth have been synchronized globally although nearly a closed packed ordering of the pores was reached (cf. plane view of pore array in Fig. 10 c)).

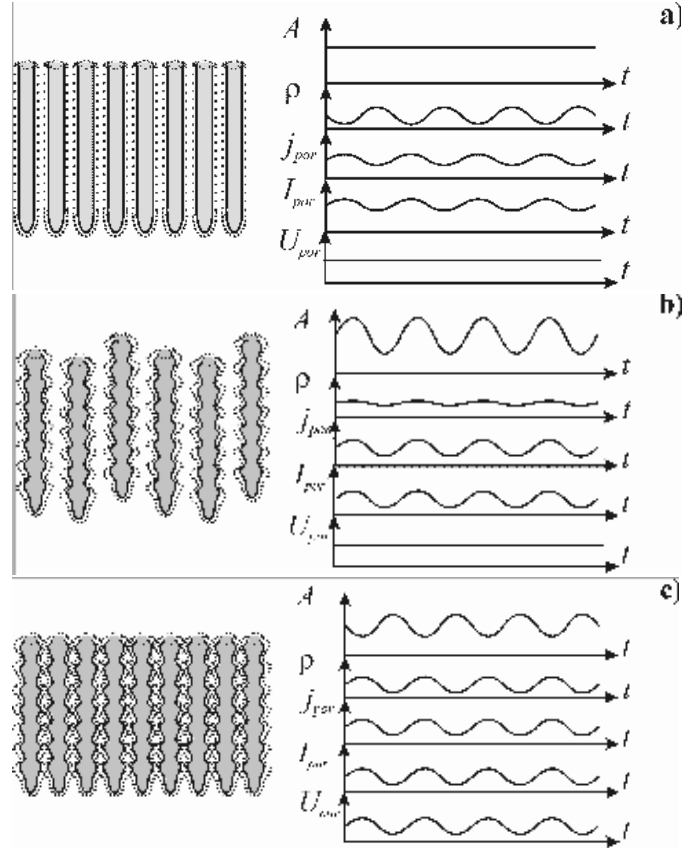


Figure 9: A schematic representation of pore interaction explaining the morphologies observed in Si and III-V compounds; a) ρ oscillates and A is constant; b) ρ is constant and A oscillates; c) ρ and A oscillate simultaneously. Note that for galvanostatic conditions a constant total current is only possible for the case of random oscillator phases.

8 Open-Loop-Control of Dynamical Systems

Contrary to the methods of Ott, Grebogi and Yorke [15] and of Pyragas [16], which allow for the stabilization of (if uncontrolled) unstable periodic orbits by parametric feedback, it may be possible to achieve stabilization even without feedback, i. e. by open-loop control. Application of non-feedback control to dynamical systems can be roughly classified into at least three classes: Addition of noise [17, 18] or of chaotic signals [19] may lead to suppression of chaos. Second, a constant (but usually large) shift in a parameter may be utilized to shift a fixed point into a parameter regime where it is stable [20]. Third, periodic parametric perturbations can be used. Counterintuitively, this is possible even by nonresonant perturbations [21]. The more straightforward approach is by resonant parametric perturbations [22, 23, 24, 25, 26, 27, 28] which in the simplest case is a weak sinusoidal signal, but can be any periodic signal. Which orbits can be stabilized by which signals in general can be investigated only if an explicit model of the system is given.

9 Open-Loop-Control of Pore Formation

For technical applications, it would be desirable to generate pores with a diameter of less than 500nm. However, at all etching conditions investigated up to now, in this diameter range always side-branching pores are obtained (cf. first row in Fig. 11).

Fortunately, the experimental setup allows for an open-loop stabilization e.g. by modulation of the intensity of illumination or by modulation of the etching current. If the modulation frequency meets the intrinsic time scale of the pore formation (0.5 min modulation in row 1), the side pore formation is hindered by the reduction of the etching current at the right phase. Which is the relevant time scale (oxide dissolution time, passivation time, ...) depends on the etching conditions and the type of pores.

Corresponding to the modulated current, the pores are regular, but with a modulated diameter (Fig. 11). The diameter modulation profile can be influenced to some extent by the waveform, nota bene these waveforms are not identical.

It should be noted, although the controlled state possibly could be considered as an instable periodic orbit of the whole etching setup, the described control method yet does not use a feedback control scheme as the OGY scheme [15]. This would be a promising extension, however, it is expected that for the case of dendritic-like sidebranching, the dynamics possibly cannot be reduced to a low-dimensional attractor.

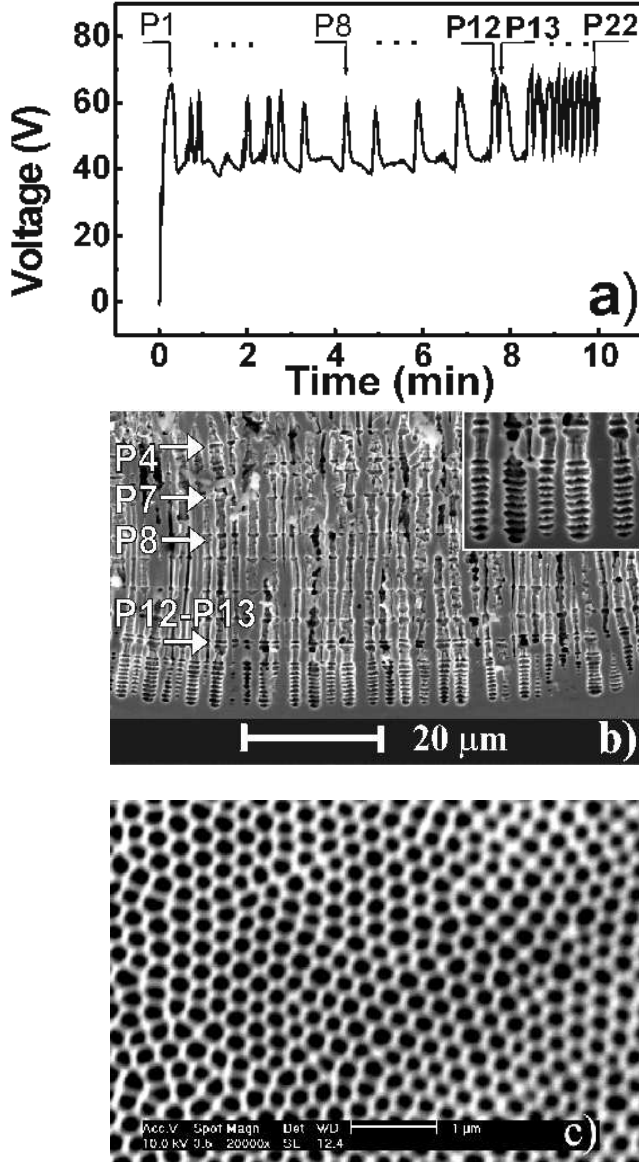


Figure 10: Data taken from an (100) oriented n-InP sample with $n_1 = 1.5 \times 10^{16} \text{ cm}^{-3}$ anodized at a constant current density $j = 100 \text{ mA/cm}^2$. The electrolyte is again HCl (5%). a) Voltage oscillations; b) cross-sectional SEM of the sample. The inset is the magnification of the nodes at the bottom of the porous layer; c) Induced by the next neighbor interaction, pores arrange into a close packed hexagonal 2D array. Correlation length is about 7 lattice constants.

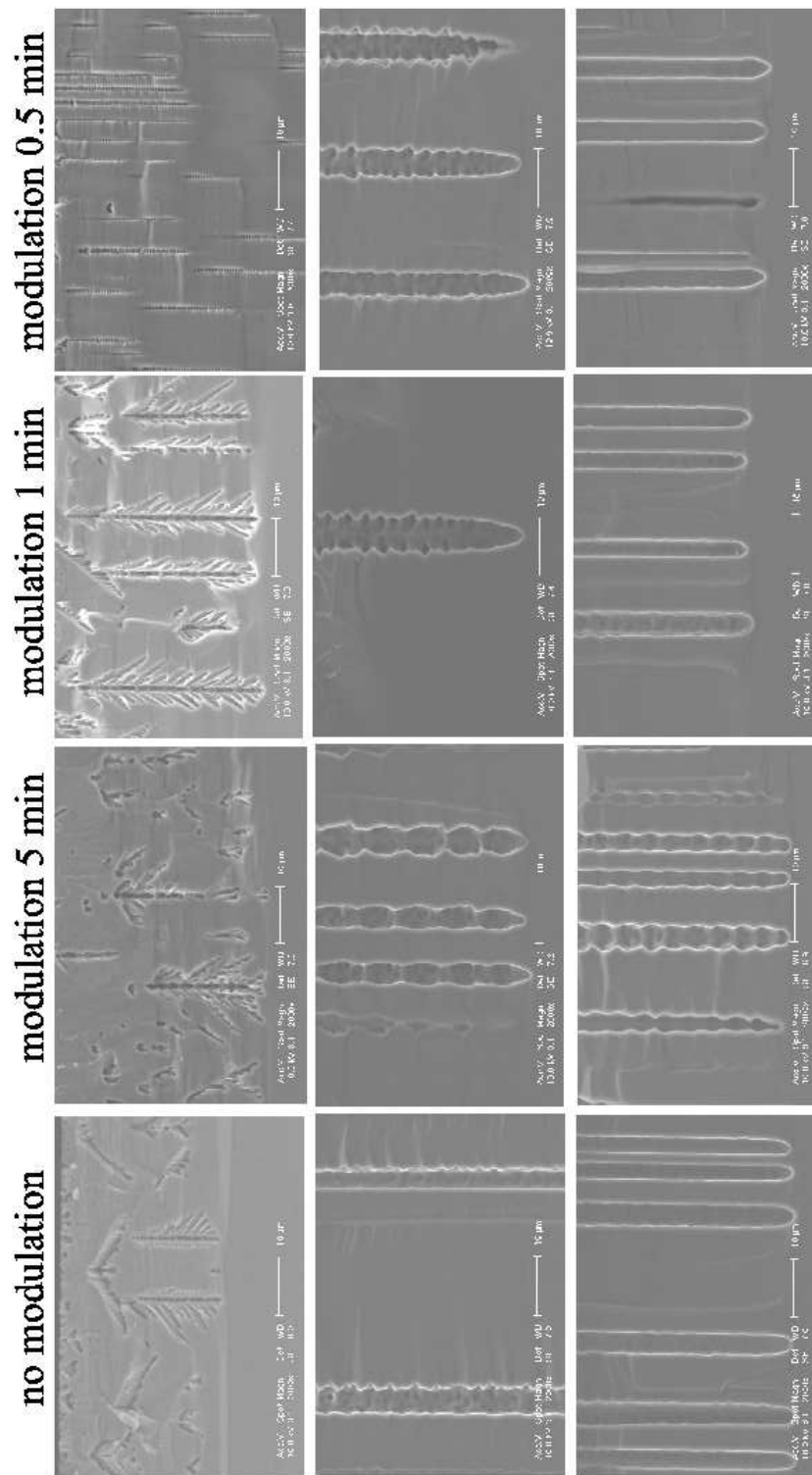


Figure 11: Branching of pores can be suppressed by an open-loop control method triggering to the system-inherent time scales (here: (100)-oriented n-Si, 1-10 Ω cm). The upper row (DMF, 4wt-% HF) corresponds to the case with less oxide generation. From middle row (H₂O, 7wt-% HF) to lower row (H₂O, 4wt-% HF), there is less oxide dissolution. In the first column the backside illumination current is constant; the triggering time decreases from 5 min in the second column to 0.5 min in the last column. Here potentiostatic conditions (4V) are used; a 20% sinusoidal modulation (with the respective period) of the current density around its average value of 4 mA/cm² is realized by control of the amplitude of backside illumination.

10 Conclusions

The Current Burst model, a local stochastic and highly nonlinear model, and the Aging concept describing the time- and orientation-dependence of the passivation behavior, provide on an intermediate level of abstraction a general approach to explain pore geometries, oscillations and synchronization with a minimum of material-dependent, but experimentally accessible, parameters. The lateral interaction of Current Bursts gives rise to synchronization phenomena, and a percolation transition to global ordering. In a technologically relevant diameter range, where one otherwise experiences excessive sidebranching of pores giving dendritic-like structures, an open-loop control can be successfully applied to suppress sidebranching of pores. To clarify quantitatively the dynamical processes in this system, and to gain detailed insight about the general controllability conditions for mesopores and perspectives for more sophisticated control strategies further experimental and theoretical efforts have to be made.

References

- [1] E. Yablonovich, D.L Allara, C.C. Chang, T. Gmitter, T.B. Bright, *Phys. Rev. Lett.*, 57, 249 (1986)
- [2] H. Föll, *Appl. Phys. A*, 53, (1991) 8
- [3] R.L. Smith, S. D. Collins, *J. Appl. Phys.*, 71, (1992) R1
- [4] Carstensen, J., Christophersen, M., Föll, H.: Pore Formation Mechanisms for the Si-HF System. *Mat. Sci. Eng. B*, **69-70** (2000) 23
- [5] Carstensen, J., Prange, R., Popkirov, G. S., Föll, H.: A model of current oscillations at the Si-HF-system based on a quantitative analysis of current transients. *Appl. Phys. A* **67-4** (1998), 459–467
- [6] Carstensen, J., Prange, R., Föll, H.: Percolation model for the current oscillation in the Si-HF system. *Proc ECS 193rd Meeting, San Diego 1998*, **98-10**, 148–157
- [7] Carstensen, J., Prange, R., Föll, H.: A model for current-voltage oscillations at the Silicon electrode and comparison with experimental results. *J. Electrochem. Soc.* 146(3), (1999) p.1134-1140
- [8] E. K. Propst, P.A. Kohl, *J. Electrochem. Soc.*, 141, (1994) 1006
- [9] E. A. Ponomarev, C. Levy-Clement, *J. Electrochem. Soc. Lett.*, 1, (1998) 1002
- [10] L. T. Canham, *Appl. Phys. Lett.*, 57, (1990) 1046
- [11] V. Lehmann, U. Gösele, *Appl. Phys. Lett.*, 58, (1991) 856
- [12] S. Langa, J. Carstensen, M. Christophersen, H. Föll, I.M. Tiginyanu, The way to uniformity in porous III-V compounds via self-organization and lithography patterning, in R. Wehrspohn (ed.), *Ordered pore structures in semiconductors*, Springer Verlag, to be published (2002)
- [13] Föll, H., Carstensen, J., Christophersen, M., Hasse, G.: A stochastic model for current oscillations in space and time at the silicon electrode. *Proceedings of the ECS fall meeting, Arizona, 2001*
- [14] Christophersen, M., Carstensen, J., Föll, H.: Macropore-formation on highly doped n-type silicon. *Phys. Stat. Sol. (a)*, 182 (1), (2000) 45
- [15] E. Ott, C. Grebogi, and J. A. Yorke, *Phys. Rev. Lett.* 64, 1196 (1990).
- [16] K. Pyragas, *Phys. Lett. A* 170, 421-428 (1992).
- [17] G. Malescio, Effects of noise on chaotic one-dimensional maps, *Phys. Lett. A* 218, 25-29 (1996).
- [18] G. D. Lythe, Dynamics controlled by additive noise, *adap-org/9708005*, *Nouvo Cimento D* 17, 855 (1995).
- [19] S. Rajasekar, *Phys. Rev. E* 51, 775 (1995).
- [20] S. Parthasarathy and S. Sinha, *Phys. Rev. E.* 51, 6239 (1995).
- [21] Y. S. Kivshar, F. Rödelsperger, and H. Benner, *Phys. Rev. E* 49, 319 (1994).
- [22] R. Lima and M. Pettini, *Phys. Rev. A* 41, 726 (1990).
- [23] G. Filatrella, G. Rotoli, and M. Salerno, *Phys. Lett. A* 178, 81-84 (1993).
- [24] R. Mettin, A. Hübler, A. Scheeline, and W. Lauterborn, *Phys. Rev. E* 51, 4065 (1995).
- [25] R. Mettin, Entrainment Control of chaos near unstable periodic orbits, p. 231-238 in: *IUTAM Symposium on Interactions between Dynamics and Control in Advanced Mechanical Systems*, ed. D. H. van Campen, *Solid Mechanics and its Applications* Vol. 52 (Kluwer Academic Publishers, Dordrecht 1997).
- [26] C. Rhodes, M. Morari, L. S. Tsimring, and N. F. Rulkov, Data-based Control trajectory planning for nonlinear systems, *Phys. Rev. E.* 56, 2398 (1997).
- [27] D. W. Sukov and D. J. Gauthier, Entraining Power-Dropout Events in an External Cavity Semiconductor Laser Using Weak Modulation of the Injection Current, *IEEE J. Quantum Electronics* 36, 175 (2000).
- [28] P. Colet and Y. Braiman, Control of Chaos in Multimode Solid State Lasers by Use of Small Periodic Perturbations, *Phys. Rev. E*, 53 200-206 (1996).